Available online at www.sciencedirect.com
SCIENCE DIRECT
Journal of Photochemistry and Photobiology A: Chemistry 181 (2006) 421–428
Journal of Photochemistry and Photobiology A:Chemistry
www.elsevier.com/locate/jphotochem

Efficient degradation of organic pollutant with WO_x modified nano TiO_2 under visible irradiation

Haiyan Song, Hongfu Jiang, Xingqin Liu, Guangyao Meng *

USTC Laboratory for Solid State Chemistry & Inorganic Membranes, Department of Materials Science and Engineering, University of Science and Technology of China (USTC), Hefei 230026, PR China

Received 15 June 2005; received in revised form 9 December 2005; accepted 7 January 2006
Available online 15 February 2006

Abstract

Nanocrystalline tungsten oxide-doped titanium dioxide (WO_x-TiO_2) powders were prepared by a sol-mixing method. The photooxidation efficiencies of WO_x-TiO_2 catalysts were evaluated by conducting a set of experiments of photodegrading Methylene blue (MB) in aqueous solution. The experiments demonstrated that the MB in aqueous solution was successfully degraded using WO_x-TiO_2 under visible light irradiation, especially when the pH value of the solution was over 6. It was found that an optimal WO_x dosage of 1% in WO_x-TiO_2 achieved the highest photocatalytic activity in the conditions of this experiment, on which MB was photooxided completely within 1 h. Powders were characterized by X-ray diffraction (XRD), X-ray photoelectron emission spectroscopy (XPS), UV–vis absorption spectra, transmission electron micrograph (TEM) measurements. These results showed that tungsten oxides not only hindered the growth of TiO_2 particles but greatly increased the transformation temperature (>800 °C) from anatase to rutile during sintering; the dominant fraction of tungsten oxides was non-stoichiometric tungsten oxide (W_xO_y) with W^{n+} ($4<n<6$), which could easily substitute Ti^{4+} in the lattice of TiO_2 because of the similarity in the ion radius of W^{n+} and Ti^{4+} to form non-stiochiometric solid solution of $W_xTi_{1-x}O_2$. The light absorption band of TiO_2 changed from the near UV to the visible light range (2.98 eV in 1.0% WO_x-TiO_2) because of the tungsten impurity energy level induced by $W_xTi_{1-x}O_2$.

Keywords: Titanium dioxide; Tungsten oxide; Methylene blue; Visible light; Impurity energy level

1. Introduction

Titanium dioxide, TiO_2, is a well-studied and commonly used material for many photocatalytic [1] and photoelectrochemical [2] applications. However, the widespread technological use of a TiO_2 photocatalyst has been hampered by its wide band gap (3.2 eV for anatase TiO_2) and the requirement of ultraviolet radiation ($A<380$ nm) for photocatalytic activation. The sun is an abundant source of photons; however, UV light accounts for only a small fraction (∼5%) compared to the visible region (45%). An efficient process that shifts the optical response of active TiO_2 from the UV to the visible spectral range can provide a framework to more easily incorporate the photocatalytic and solar efficiency of this material [3].

Several attempts have been made to convert the TiO_2 adsorption onset from the ultraviolet to the visible region by doping transition metals [4–7]. However, metal doping has several drawbacks: the doped materials have been showed to suffer from thermal instability, and the metal centers act as electron traps, which reduce the photocatalytic efficiency. Furthermore, the preparation of transition-metal-doped TiO_2 requires very expensive ion-implantation facilities [8,9]. Recently, it is shown that the desired band gap narrowing of TiO_2 can be better achieved by using anionic dopants rather than metal ions [3,10–12], and substitutional doping of nitrogen is found to be most effective because its p states contribute to the band gap narrowing by mixing with O 2p states [3]. Nevertheless, the doping processes such as that TiO_2 films is doped with nitrogen by sputtering method and that TiO_2 powder is annealing at elevated temperature under NH_3 flow for several hours are all physical methods and the equipments required are very expensive. Li et al. [13] have prepared WO_x-TiO_2 samples by a sol–gel process with the aims of extending the light

* Corresponding author. Tel.: +86 551 3603234; fax: +86 551 3607627.
E-mail address: mgym@ustc.edu.cn (G. Meng).

1010-6030/$ – see front matter © 2006 Elsevier B.V. All rights reserved.
doi:10.1016/j.jphotochem.2006.01.001

absorption spectrum toward the visible region, but the photocatalytic activity of the samples is not satisfying because of some reasons.

In the present study, WO_x-TiO_2 samples were prepared by a novel sol-mixing process to enhance the photocatalytic activity in the visible light region. Methylene blue (MB) can be degraded completely on the WO_x-TiO_2 system under visible light within 1 h.

2. Experimental

2.1. Synthesis of WO_x-TiO_2 catalysts

The WO_x-TiO_2 catalysts with different WO_x fraction were synthesized by sol-mixing process. TiO_2 transparent sol was first prepared via controlled hydrolysis of titanium tetrabutoxide. In a typical experiment, 5 ml of Ti $(OC_4H_9)_4$ dissolved in 34 ml anhydrous ethanol (with 2 ml acetic acid added to control the hydrolysis of Ti $(OC_4H_9)_4$), then, 2 ml distilled water was added dropwise to the solution above, which was adjusted to pH 3.0 with nitric acid; the H_2WO_4 sol was prepared as follows: HCl (20 ml, 0.7 M) was added drop by drop to a Na_2WO_4 solution (100 ml, 0.03 M) under magnetic stirring. A transparent aqueous sol was obtained, which was closed in a dialytic membrane pipe and dialytic put in a 1000-ml beaker containing deionized water for a period of 6 h. The deionized water was periodically replaced until Cl^- ions could not be detected by $AgNO_3$. A final transparent H_2WO_4 sol was thereby achieved; then the H_2WO_4 sol of suitable volume was added drop by drop to the TiO_2 sol under stirring at the WO_x/TiO_2 molar ratio of 0.5, 1.0, 2.0 and 4.0%. The resulting colloidal mixture was dried at 70 °C until the solvent being evaporated completely, and then subjected to heat treatments at various temperatures for 3 h. All the chemicals used in this study were of analytic grade.

2.2. Characterization of photocatalysts

X-ray powder diffraction (XRD) patterns of the photocatalysts were obtained using a Philip X'pert diffractometer with Cu Kα radiation (λ = 1.54187 nm). The accelerating voltage and the applied current are 40 kV and 40 mA, respectively. Crystallite sizes were calculated from the peak widths using the Scherrer equation:

$$D = \frac{k\lambda}{\beta \cos\theta} \quad (1)$$

where D is the crystallite size, k a shape factor (a value of 0.89 was used in this study), λ the X-ray radiation wavelength (1.54187 Å for Cu Kα) and β is the half width of the peak at 2θ.

The specific surface area was determined by a ST-03 A device. The samples were degassed at 200 °C for 2 h and the adsorbate gas consisted of a mixture of 30% N_2/70% He. A Hitachi, H600-II transmission electron microscope (TEM) was used to observe the morphology and determine the particle sizes. The UV–vis absorption spectra of the samples were measured in the range of 250–700 nm using a UV–vis Spectrophotometer (Shimadzu UV-2401PC). And the concentrations of the Methylene blue were also determined by the Spectrophotometer in the range of 190–800 nm. Elemental composition and valence state of the photocatalysts were analyzed by X-ray photoelectron spectroscopy (XPS) (Escalab MKII) using the Mg Kα as a radiation source.

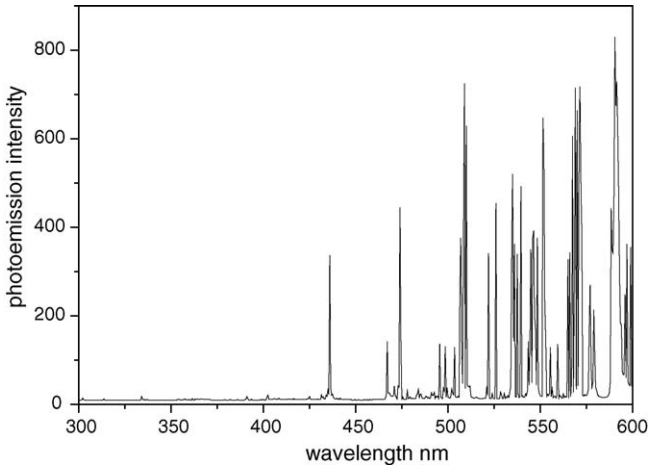

Fig. 1. The photoemission spectra of the halogen lamp.

2.3. Evaluation of photocatalytic activity

In the present study, a 175 W metal halide lamp (Ya Ming, Shanghai) was used, which was positioned over the vessel surrounded by a circulating water jacket to cool the reacting solution. The halogen lamp was equipped with a cut-off filter to completely remove any radiation below 420 nm and thus to ensure illumination by visible light only. The photoemission spectrum of the light source is illustrated in Fig. 1.

Reaction suspensions were prepared by adding 0.3 g photocatalyst powder into a 300 ml aqueous Methylene blue solution with an initial concentration of 10 mg/l. Prior to photooxidation, the suspension was magnetically stirred in a dark condition for 30 min to establish an adsorption–desorption equilibrium condition. The aqueous suspension containing MB and photocatalyst were irradiated under the visible light with constant stirring. At the given time intervals, analytical samples were taken from the suspension and immediately centrifuged at 1000 rps for 5 min, the filtrate was then analyzed by UV–vis Spectrophotometer.

The photodegradation reactions of chloroform under UV light were carried out in a 600 ml cylindrical glass vessel with a 4-W UV lamp (wavelength: 365 nm) placed at the axis of the vessel. The lamp is installed into a quartz glass tube to protect from direct contact with the aqueous solution. The tests were always performed with $[TiO_2] = 0.2$ g/l, $[CHCl_3]_0 = 1$ mmol/l, The catalysis reactivity of the samples for $CHCl_3$ photodegradation was defined as degradation yield after irradiating the solution. The yield was determined by measuring the Cl^- concentration by using a chloride ion selective electrode.

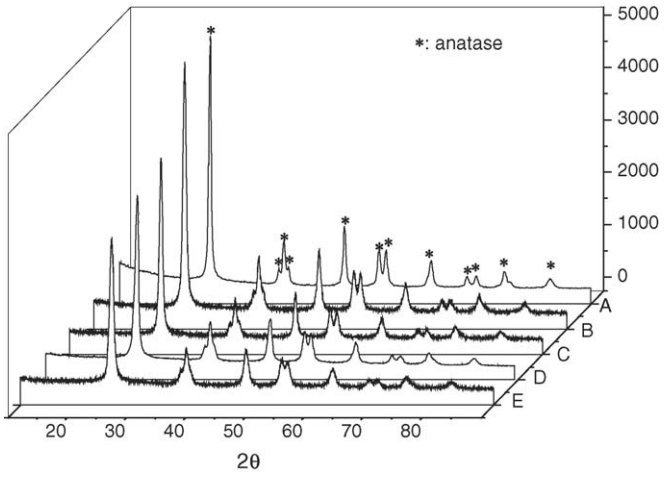

Fig. 2. XRD patterns of pure TiO_2 and WO_x-doped TiO_2 samples calcined at 500 °C for 3 h. (A) Pure TiO_2; (B) 0.5% WO_x-TiO_2; (C) 1% WO_x-TiO_2; (D) 2% WO_x-TiO_2; (E) 4% WO_x-TiO_2.

3. Results and discussion

3.1. XRD analysis

XRD patterns of pure TiO_2 and WO_x-doped TiO_2 samples calcined at 500 °C for 3 h are shown in Fig. 2. For all of the samples, no other phases were detected except anatase, it may be concluded that W^{n+} ($4<n<6$) substitute Ti^{4+} in the lattice of TiO_2 because of the similarity in the ion radius of W^{n+} (0.62–0.70 Å) and Ti^{4+} (0.68 Å) to form non-stiochiometric solid solution of $W_xTi_{1-x}O_2$ that could lead to produce a tungsten impurity energy level as described in [13].

It can also be seen from the Fig. 2 that the diffraction peaks broadened with the increase of WO_x. The particle sizes and specific surface areas that well matched the particle sizes determined by TEM are listed in Table 1. It can be seen that the WO_x-TiO_2 samples had increased specific areas and finer particle sizes compared with pure TiO_2 catalyst, this is one of the reasons to enhance the photocatalytic behavior of tungsten oxide modified TiO_2.

Fig. 3 is the XRD patterns of pure TiO_2 and 1% WO_x-TiO_2 samples calcined at temperatures from 600 to 800 °C for 3 h. The spectrum results indicated that pure TiO_2 samples underwent a phase transformation from anatase to rutile during sintering treatment. Higher sintering temperature formed more rutile phase. While for the 1% WO_x-TiO_2 samples, the results showed that all the samples almost contained none of rutile phase even after sintering at 800 °C for 3 h. Obviously, tungsten oxides hindered the transformation from anatase to rutile during sintering.

Table 1
Particle size and specific surface area of photocatalysts

Samples	Particle size (nm)	Specific surface area (m^2/g)
TiO_2	6.47	74.301
0.5% WO_x/TiO_2	4.24	80.658
1.0% WO_x/TiO_2	3.63	89.223
2.0% WO_x/TiO_2	3.00	97.586
4.0% WO_x/TiO_2	2.45	102.231

All the samples were calcined at 500 °C for 3 h.

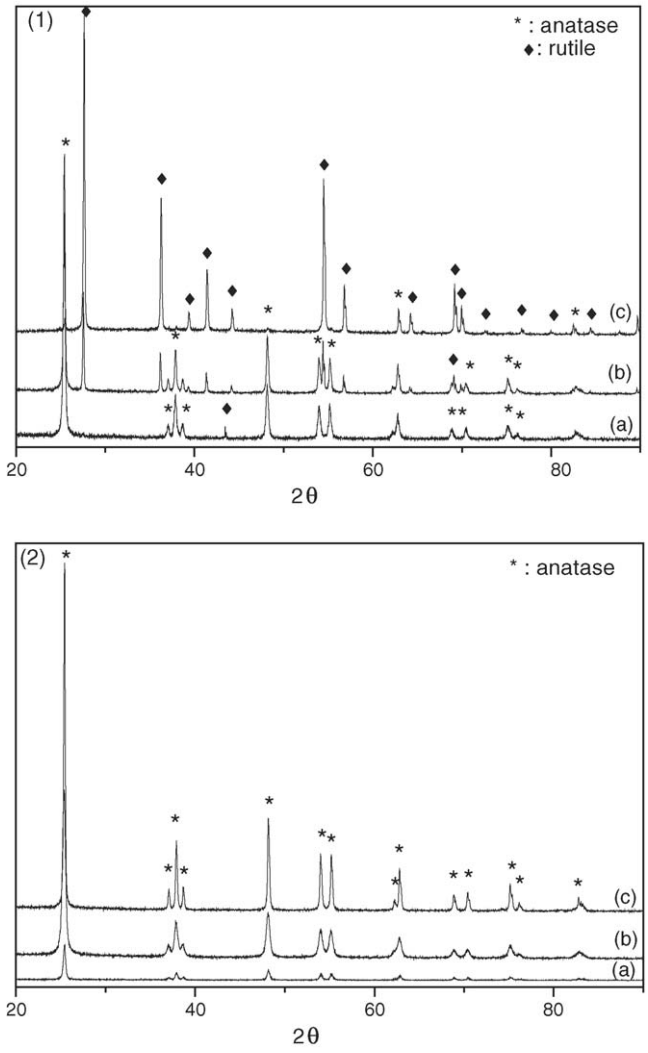

Fig. 3. XRD patterns of pure TiO_2 (1) and 1% WO_x-TiO_2 (2) powders calcined at different temperatures for 3 h: (a) 600 °C; (b) 700 °C; (c) 800 °C.

3.2. XPS analysis

The XPS analysis was carried out to determine the chemical composition of the catalysts and the valence states of various species present therein. The XPS data of O 1s, Ti 2p and W 4f and their valence states obtained from fitted curves are shown in Table 2. The Ti 2p XPS spectra and the valence states of pure and doped TiO_2 samples are illustrated in Fig. 4A. For the pure TiO_2, the Ti 2p peaks are narrow and have a binding energy of 458.25 eV (FWHM = 1.49 eV), attributed to Ti^{4+}. For the 1% WO_x-TiO_2, the spectrum appears in a wide range (FWHM = 1.57 eV) and its intensity decreases, perhaps due to tungsten oxides being doped in the lattice of TiO_2. The binding energy was 0.25 eV, less than that of pure TiO_2. These results had a good agreement with those in [13].

For the pure TiO_2, the O 1s peak was also narrow with slight asymmetry as described in Fig. 4B, two peaks were

Table 2
XPS data and their valence states obtained from the fitted curves

Catalysts	TiO_2			1% WO_x-TiO_2		
	Binding energy (eV)	FWHM[a] (eV)	Area (%)	Binding energy (eV)	FWHM* (eV)	Area (%)
O 1s	529.60	1.63	76.52	529.75	1.90	48.00
O 1s	531.05	1.78	23.48	531.50	1.90	20.90
O 1s				530.74	2.54	11.07
O 1s				532.98	1.52	19.97
Ti 2p	458.25	1.49	100.00	458.00	1.57	100.00
W 4f				34.90	2.10	31.57
W 4f				36.50	1.84	59.44
W 4f				37.64	2.06	8.99

[a] FWHM: full width at one-half of the maximum height of peaks.

obtained by fitting the curve. A dominant peak at 529.6 eV (FWHM = 1.63 eV) was attributed to TiO_2, and the other peak much smaller at 531.05 eV was attributed to the hydroxyl adsorbed on the surface of TiO_2. While, the O 1s XPS spectra showed a four-band structure for the 1% WO_x-TiO_2 in Fig. 4C and Table 2. Similarly, the peaks at 529.75 and 531.5 eV were attributed to TiO_2 and the hydroxyl adsorbed on the surface of the catalyst, respectively; the peak at 530.74 eV was attributed to WO_3 and the peak at 532.98 eV agreed with the O 1s electron binding energy for WO_x molecule. The O 1s peaks of 1% WO_x-TiO_2 were smaller than that of TiO_2 due to WO_x being doped on the surface of TiO_2. The peak area proportion of O 1s for hydroxyl in 1% WO_x-TiO_2 was larger than that in pure TiO_2. As Linsebigler et al. [14] reported, hydroxyl would combine with the surface-trapped hole to form $^{\bullet}OH$ radical that have strong oxidation activity. This is another reason for which TiO_2 doped with WO_x has higher photocatalytic activity than that of pure TiO_2.

The W 4f XPS spectra are shown in Fig. 4D. The fitting analysis indicated that the tungsten in the 1% WO_x-TiO_2 might present in the mixed valence of W^{4+} (31.57%), W^{n+} (59.44%) and W^{6+} (8.99%). The results showed that the dominant fractions of tungsten oxides were non-stoichiometric tungsten oxides (W_xO_y) and WO_2, while the WO_3 was very little. This result is contrary

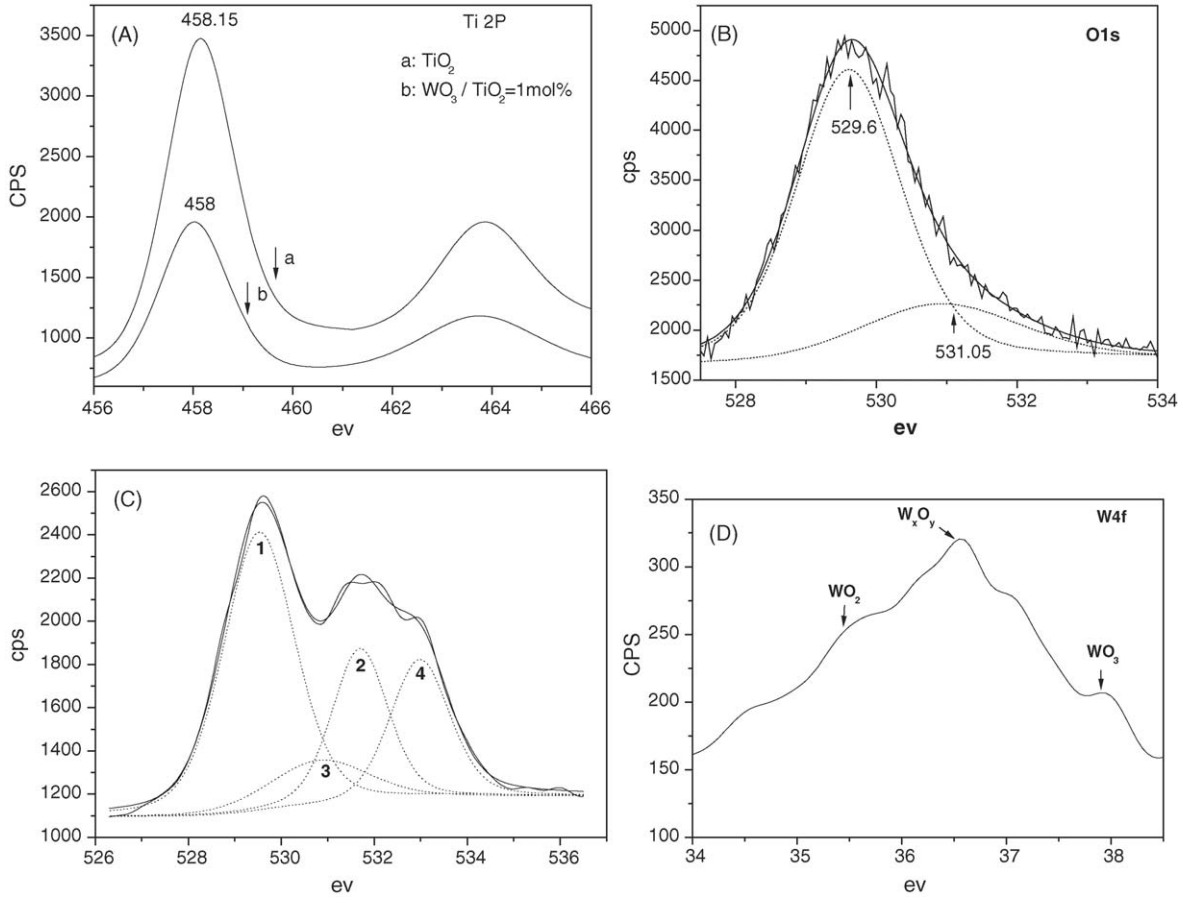

Fig. 4. XPS fitting spectra of pure TiO_2 and 1% WO_x-TiO_2 powders. (A) Ti 2p; (B) O 1s of TiO_2; (C) O 1s of 1% WO_x-TiO_2; (D) W 4f.

to the report of [13]. Vermaire and van Berge [15] proposed that the stoichiometric ion exchange between W^{4+} and Ti^{4+} might occur. In fact, W^{n+} can substitute Ti^{4+} in the lattice of TiO_2 because of the similarity in the ion radius of W^{n+} and Ti^{4+}. So, non-stiochiometric solid solution of $W_xTi_{1-x}O_2$ would form that could lead to produce a tungsten impurity energy level, as described thereinafter.

3.3. Photocatalytic oxidation

The efficiency of photocatalytic oxidation using the WO_x-TiO_2 samples was evaluated on the basis of the photodegradation percent of MB in aqueous solution. The photodegradation percent of MB using pure TiO_2 and the TiO_2 doped with 0.5, 1, 2, 4 and 6% WO_x are illustrated in Fig. 5a. For each catalyst, five samples were collected at the time intervals of 15 min after the irradiation of 1 h, the photodegradation percent of MB was achieved to 38.5, 85.2, 98.0, 73.5, 50.9 and 36.8%, respectively. It was found that the WO_x impurity doped in TiO_2 could enhance the photocatalytic activity of TiO_2 significantly. While the impurity fraction of WO_x in TiO_2 increased, the rate of MB photodegradation increased initially and then decreased when the WO_x content exceeds 1%. This implies there was an optimum molar content of $WO_x = 1\%$. Fig. 5b is the UV–vis absorption spectra of MB before and after photodegradation using 1% WO_x-TiO_2 catalyst. It was clear that the characteristic absorption peak at 650 nm of MB weakened with the catalytic reaction going on, and after irradiating for 1 h, the absorption peak disappeared completely. At the same time, the absorption peak at the UV range of MB weakened greatly, which means that under the visible right, the MB was not only discolored completely but also could be oxidized greatly to form carbon dioxide and water. The removal percent of TOC was achieved to 93.6% using 1% WO_x-TiO_2 catalyst. Fig. 6 is the comparison of the photocatalytic decomposition of MB under visible light in the present of doped N [16], C [17] and WO_x titania nanoparticles. It is concluded that the TiO_2 doped with WO_x prepared by sol–gel process is efficient under visible light irradiation.

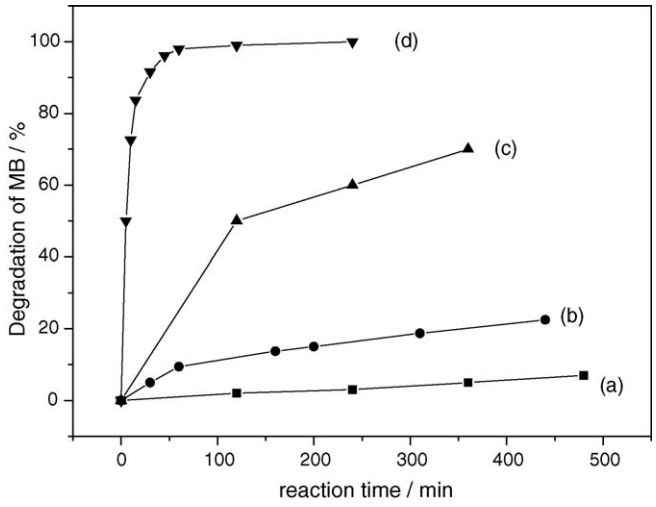

Fig. 6. Comparison of the photocatalytic decomposition of MB under visible light without any catalyst (a) and in the present of titania nanoparticles doped with N (b), C (c) and 1 mol% WO_x (d).

Because MB are readily degraded by UV light without any catalysts, we investigated the photocatalytic activity of TiO_2 and WO_x-TiO_2 for $CHCl_3$ that is a colorless organic compound degradation at $\lambda = 365$ nm. The results were shown in Fig. 7, the photocatalytic activity of WO_x-TiO_2 under UV light increased with the increase of the impurity fraction of WO_x and then decreased when the WO_x content exceeds 1 mol%, which can be explained that when the fraction of WO_x is less than 1 mol%, the WO_x-TiO_2 samples had increased specific areas and finer particle sizes compared with pure TiO_2 catalyst that is the important reason to enhance the photocatalytic behavior of WO_x-TiO_2. On the other while, the tungsten impurity energy level induced by $W_xTi_{1-x}O_2$ may be an electron–hole recombination center under the UV irradiation when the WO_x content exceeds 1%.

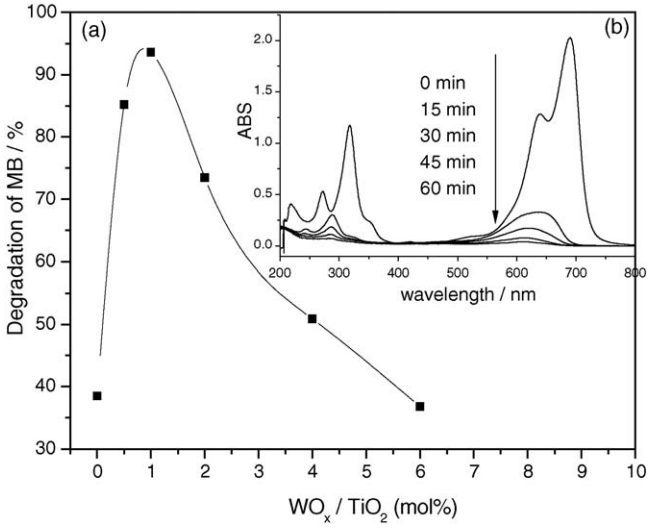

Fig. 5. (a) The affection of molar ratio of WO_x on the degradation of MB. (b) The UV–vis absorption spectra of MB before and after photodegradation using 1% WO_x-TiO_2 catalyst.

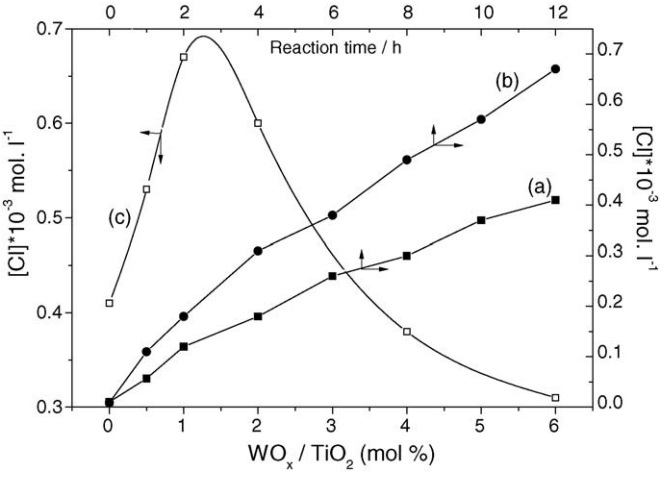

Fig. 7. Photocatalytic activity of TiO_2 (a) and WO_x-TiO_2; (b) for $CHCl_3$ degradation at $\lambda = 365$ nm; (c) the affection of molar ratio of WO_x on the degradation of MB under UV light.

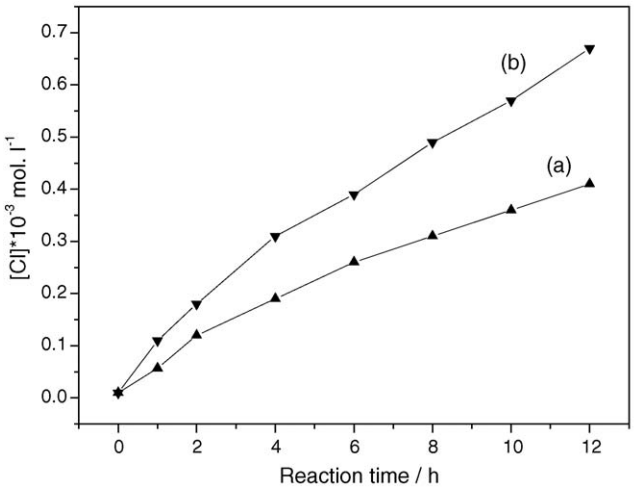

Fig. 8. Photocatalytic degradation of $CHCl_3$ under visible light (>420 nm) on the catalysts (a) TiO_2 + MB and (b) WO_x-TiO_2 + MB.

The photocatalytic activity of TiO_2 and WO_x-TiO_2 for $CHCl_3$ degradation under visible light shown in Fig. 8 were also evaluated. The photocatalytic activity of TiO_2 and WO_x-TiO_2 for $CHCl_3$ degradation is lower than that for MB degradation. When 3 mg MB was added to the reaction systems, the quantum yields of catalysts increased and were almost equal to that of catalysts irradiated by UV light. These results indicated that the higher activity of TiO_2 and WO_x-TiO_2 was attributed to the visible light absorbed by MB that in fact acts as a photosensitive compound for the catalysts [18].

Therefore, the photocatalytic activities of WO_x-TiO_2 (A) and pure TiO_2 (B) for $CHCl_3$ degradation in the absence of MB under different light irradiation were studied (Fig. 9). The light of halogen lamp was cut by some color filters to produce two kinds of the visible light source, regions I (>420 nm) and II (>460 nm). Sample A has the higher catalytic activity than that of B during UV light irradiation due to its increased specific areas and finer particles sizes, which were stated above. Under the irradiation of the region I light, the degradation of $CHCl_3$ on samples A and B was observed. For sample B, which does not absorb the majority of this region, the catalytic activity decreased notably. Because sample B cannot be photoexcited by the region II light, this light did not degrade the $CHCl_3$ on sample B, on the other hand, sample A, exhibiting the opticle absorption at wavelengths of <650 nm, showed a high photocatalytic activity even in region II.

In the experimental process, the H_2WO_4 sol was dialyzed in a dialytic membrane pipe to remove the Na^+. To study the affection of Na^+ on the photocatalytic activity of the WO_x-TiO_2 samples, a mixed sol was prepared by adding H_2WO_4 sol without dialysis to TiO_2, then dried and calcined at 500 °C; the obtained sample was named TWN. Compared with the 1% WO_x-TiO_2 catalyst, the photocatalytic activity of TWN abated due to the existence of Na^+. In fact, a prerequisite for high photocatalytic activity of TiO_2 may involve the possibility of charge pair generation and migration to the surface of previously trapped charges. Thus we conclude that Na^+ is an efficient charge pair recombination center.

3.4. Iso-electric point and affection of pH values

Fig. 10 is the dependence of pH values of aqueous on photocatalytic activity of the 1% WO_x-TiO_2 catalyst. It could be seen from the curve that when pH < 6, the catalytic activity increased with increasing of the pH value; when pH 6–7, the catalyst had a highest catalytic activity that kept steady when pH > 7. This phenomenon can be attributed to the adsorbability of MB on the surface of the catalyst. In fact, the photocatalytic process mainly occurs on the photocatalyst surface, but not in bulk solution. The adsorption of substrates is indispensable for their photocatalytic degradation. It is believed that the iso-electric point would greatly influence the adsorption of organic substrates and its intermediates on the surface of photocatalyst during photoreaction. The zeta (ζ) potentials of 1% WO_x-TiO_2 sample were measured in the pH range of 2.0–9.0, and the iso-electric point of the sample was determined as around pH 5.4 as shown in Fig. 9. As a cationic dye, MB will be repulsed away from the surface of the catalyst particles on which there are positive charges in the acidic aqueous. On the contrary, when the pH value is higher

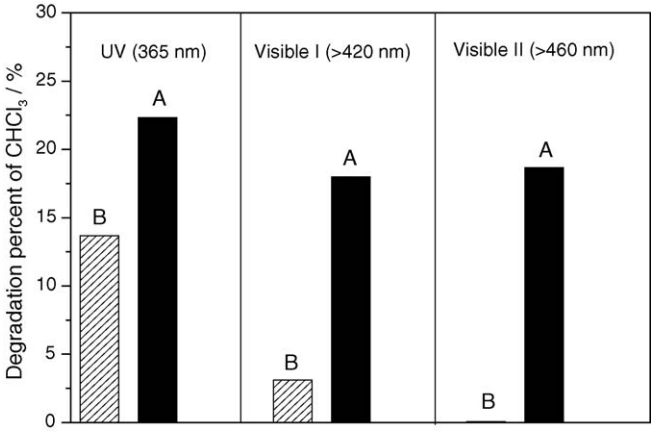

Fig. 9. Degradation percent of $CHCl_3$ on the photocatalysts WO_x-TiO_2 (A) and pure TiO_2 and (B) under different light irradiation. Reaction time: 12 h.

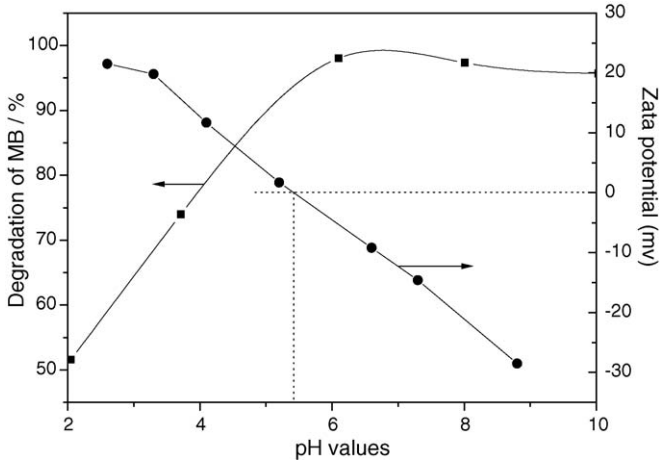

Fig. 10. Photocatalytic activities and zeta potentials of 1% WO_x-TiO_2 catalyst at different pH values.

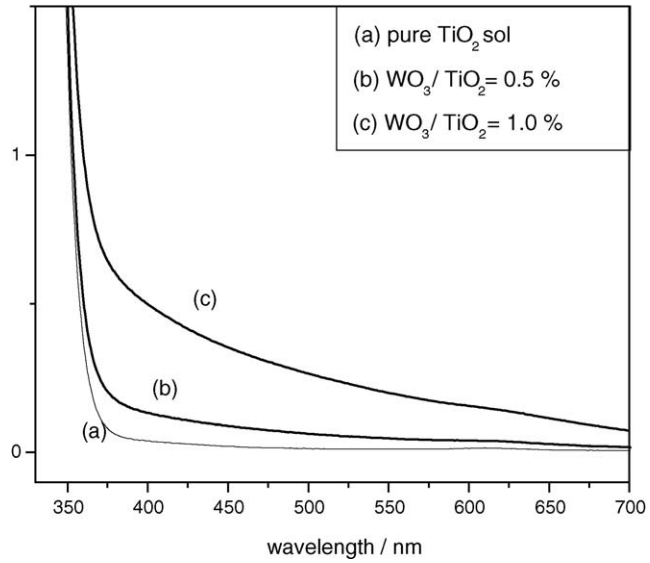

Fig. 11. (a–c) The UV–vis optical absorption spectra of pure TiO_2 and WO_3-TiO_2 sols.

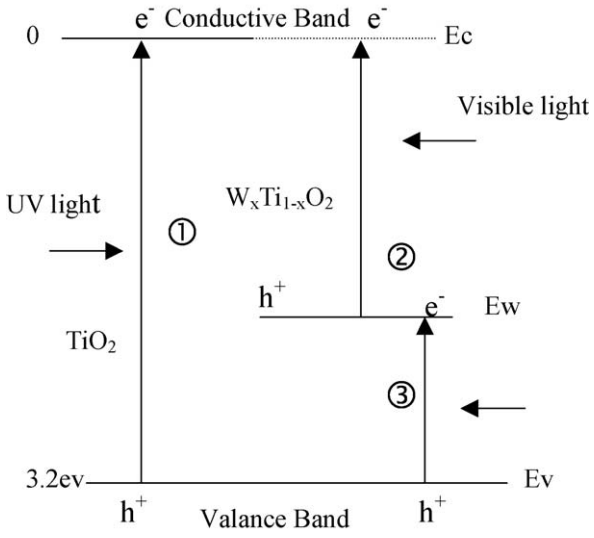

Fig. 12. Energy diagram for TiO_2 and WO_x-TiO_2 systems.

than the iso-electric point of the catalyst, the charges on the surface are negative, thus, MB can be attracted on the surface of the catalyst particles easily, which will promise the high catalytic activity of the catalyst.

3.5. Optical adsorption

Fig. 11 shows the absorption spectra of the pure TiO_2 and WO_3-doped TiO_2 sol. It is clear that the WO_3-TiO_2 samples had a better optical absorption in the region of 400–700 nm owing to the presence of tungsten oxides than pure TiO_2. Although no clear optical absorption peak in the visible region was observed, the optical absorption edges significantly shifted to red direction. With regard to the relationship between the absorption coefficient α and the incident photon energy $h\nu$ near the band edge, one can write out a good approximation [19]:

$$\alpha(h\nu) \propto (h\nu - E_g)^{n/2} \quad (2)$$

For samples in the aqueous sol, that is amorphous TiO_2, the absorption coefficient α is known to obey Eq. (2) with $n = 3$ [19]. Therefore, the band edges (E_g) of TiO_2 sol can be determined from the corresponding absorption curves as 3.34 eV, which is higher than that of the bulk band gap (3.20 eV), the result is in good agreement with the predictions of the quantum size effect [14], which means that E_g shifts to higher energy when the mean size of the nanoclusters decreases. From Fig. 11, the band edge gradually decreases with adding more and more WO_3 nanoclusters, as compared with the original TiO_2 aqueous sol. The band edges of 0.5% WO_3-TiO_2 and 1.0% WO_x-TiO_2 sols determined from the Eq. (2) are 2.90 and 2.68 eV, respectively.

Thus, it was concluded from the change of light absorption band from the near UV to the visible light range and the results of XRD and XPS that a complex of $W_xTi_{1-x}O_2$ formed in TiO_2 doped with tungsten oxides, which had a lower energy level (2.98 eV in 1.0% WO_x-TiO_2) than that of TiO_2 as shown in Fig. 12. When $h\nu \geq (E_c - E_v)$, electrons can be excited in the valence band of TiO_2; when $(E_c - E_w) \leq h\nu < (E_c - E_v)$, electrons can be excited from the $W_xTi_{1-x}O_2$ energy level, and when $(E_w - E_v) \leq h\nu < (E_c - E_w)$, electrons can be excited from the valence band of TiO_2 to the $W_xTi_{1-x}O_2$ energy level.

4. Conclusions

The photocatalysts of WO_x-TiO_2 were prepared by a sol-mixing method and characterized by XRD, XPS, TEM and UV–vis absorption spectra. The following results can be concluded:

1. WO_x not only hindered the growth of TiO_2 particles but also greatly increased the transformation temperature (>800 °C) from anatase to rutile during sintering.
2. The dominant fraction of tungsten oxides was W_xO_y with W^{n+} ($4 < n < 6$), which could substitute Ti^{4+} in the lattice of TiO_2 because of the similarity in the ion radius of W^{n+} and Ti^{4+} to form non-stiochiometric solid solution of $W_xTi_{1-x}O_2$ that could lead to produce a tungsten impurity energy level.
3. The light absorption band of TiO_2 changed from the near UV to the visible light range (2.68 eV in 1.0% WO_x-TiO_2) because of the tungsten impurity energy level.

Acknowledgement

The authors are grateful to the Ministry of Science and Technology of China for financial support (No. 2003CB615700).

References

[1] A. Fujishima, K. Hashimoto, T. Watanabe, TiO_2 Photocatalysis, Bkc, Inc., Tokyo, Japan, 1999.
[2] A. Hagfeldt, M. Gräted, Acc. Chem. Res. 33 (2000) 269.
[3] R. Asahi, T. Morikawa, T. Ohwaki, K. Aoki, Y. Taga, Science 293 (2001) 269.
[4] A.K. Ghosh, G.P. Maruska, J. Electrochem. Soc. 24 (1977) 1516.
[5] W. Choi, A. Termin, M.R. Hoffmann, J. Phys. Chem. 98 (1994) 13669.

[6] M. Anpo, Catal. Surveys Jpn. 1 (1997) 169.
[7] J. Akikusa, Thesis, Duquesne University, 1997.
[8] Y. Wang, H. Cheng, Y. Hao, J. Ma, W. Li, S. Cai, Thin Solid Films 349 (1999) 120.
[9] H. Yamashita, M. Honda, M. Harada, Y. Ichihashi, M. Anpo, T. Hirao, N. Itoh, N.J. Iwamoto, Phys. Chem. B 102 (1998) 10707.
[10] H. Irie, Y. Wanatabe, K.J. Hashimoto, Phys. Chem. B 107 (2003) 5483.
[11] J.C. Yu, J.G. Yu, W.K. Ho, Z.T. Jiang, L.Z. Zhang, Chem. Mater. 14 (2002) 3808.
[12] S.U.M. Khan, M. Al-Shahry, W.B. Ingler Jr., Science 297 (2002) 2243.
[13] X.Z. Li, F.B. Li, C.L. Yang, W.K. Ge, J. Photochem. Photobiol. A: Chem. 141 (2001) 209.
[14] A.L. Linsebigler, G.Q. Lu, J.T. Yates, Chem. Rev. 95 (1995) 735.
[15] D.C. Vermaire, P.C. van Berge, J. Catal. 116 (1989) 309.
[16] C. Burda, Y.B. Lou, X.B. Chen, A.C.S. Samia, J. Stout, J.L. Gole, Nano Lett. 3 (2003) 1049.
[17] Sh. Sakthivel, H. Kisch, Angew. Chem. Int. Ed. 42 (2003) 4908.
[18] M. Mrowetz, W. Balcerski, A.J. Colussi, M.R. Hoffmann, J. Phys. Chem. B 108 (2004) 17269.
[19] E.J. Johnson, in: R.K. Willardson, A.C. Beer (Eds.), Semiconductors and Semimetals, vol. 3, Academic Press, New York, 1967 (Chapter 6).